Adiabatic and non-adiabatic small-polaron hopping conduction in $La_{1-x}Pb_xMnO_{3+\delta}$ ($0.0 \leq x \leq 0.5$)-type oxides above the metal–semiconductor transition

2001 J. Phys.: Condens. Matter 13 9489

(http://iopscience.iop.org/0953-8984/13/42/310)

INSTITUTE OF PHYSICS PUBLISHING JOURNAL OF PHYSICS: CONDENSED MATTER

J. Phys.: Condens. Matter **13** (2001) 9489–9504 PII: S0953-8984(01)19858-9

Adiabatic and non-adiabatic small-polaron hopping conduction in $La_{1-x}Pb_xMnO_{3+\delta}$ ($0.0 \leqslant x \leqslant 0.5$)-type oxides above the metal–semiconductor transition

Aritra Banerjee[1], Sudipta Pal[1], E Rozenberg[2] and B K Chaudhuri[1,3]

[1] Solid State Physics Department, Indian Association for the Cultivation of Science, Calcutta-700032, India
[2] Department of Physics, Ben-Gurion University of the Negev, PO Box 653, Beer-Sheva 84105, Israel

E-mail: sspbkc@mahendra.iacs.res.in

Received 7 December 2000
Published 5 October 2001
Online at stacks.iop.org/JPhysCM/13/9489

Abstract

Above the semiconductor-to-metallic transition (SMT) temperature (T_p), transport properties of the $La_{1-x}Pb_xMnO_{3+\delta}$ ($0 \leqslant x \leqslant 0.5$)-type mixed valence oxides with T_p between 230 and 275 K (depending on x) have been thoroughly examined for a small-polaron hopping conduction mechanism of the carriers. Although the variable range hopping (VRH) model was used earlier to fit the entire conductivity data above SMT, we noticed two distinct regions (above and below $\theta_D/2$; θ_D is the Debye temperature) where different types of conduction mechanisms are followed. The high temperature ($T > \theta_D/2$) conductivity data of all the Pb-doped samples follow the adiabatic hopping conduction mechanism, while those of $LaMnO_3$ ($x = 0$) showing no SMT follow the non-adiabatic hopping conduction mechanism of Mott or Emin with reasonable values of polaron radius, hopping distance, polaron binding energy, activation energy, etc being different for different systems. The VRH model, however, fits the corresponding low temperature ($T < \theta_D/2$) data of all the samples. Both resistivity $\rho(T)$ and thermoelectric power $S(T)$ follow a similar microscopic theory above T_p supporting the small-polaron hopping mechanism. Thermoelectric power also showed appreciable magnetic field dependence around SMT.

1. Introduction

In recent years perovskite-type oxide materials of composition $La_{1-x}A_xMnO_{3+\delta}$ (with A = Sr, Ca, Ba, etc) have drawn considerable attention from theoretical and experimental researchers

[3] Author to whom correspondence should be addressed.

[1–6] because of their interesting negative magnetoresistive behaviour and other temperature-dependent non-linear physical properties. The electrical conductivity and antiferromagnetic properties of such perovskites were explained in terms of the double-exchange interaction [7], i.e. the transfer of electrons between Mn^{3+} and Mn^{4+} ions. Thermopower (S) and resistivity (ρ) data [5] on such rare-earth manganates have shown evidence in favour of the formation of small polarons. This is because of the fact that these oxides contain mixed-valence transition metal ions (TMI) and hopping/tunnelling from the higher to the lower valence states of the TMI occurs. Recently, specific heat and resistivity studies by Park *et al* [8] on $La_{0.7}Ca_{0.3}MnO_3$ also indicated the formation of polarons in this system. The small polaron effect can also be attributed to the large difference in ionic size (20%) between Mn^{3+} and Mn^{4+} ions [9].

Polaron hopping theory [10, 11] was originally used to explain transport in doped or undoped semiconductors where electrons occupying hydrogenic orbitals with wavefunction $\varphi = \varphi_0 \exp(-2\alpha R)$ are localized by potential fluctuations associated with the dopant. There is a competition between the potential energy difference and the distance electrons can hop. This is reflected in the expression of the hopping rate (η) to a site at a distance R where the energy of the carrier is ΔW higher than that at the origin:

$$\eta = \eta_0 \exp(-2\alpha R) \exp(-\Delta W/kT) \tag{1a}$$

This expression is identical to the small-polaron hopping model of Mott [12] (shown in section 2), since η is proportional to the conductivity (σ). The variable range hopping (VRH) model (generally applicable in the low temperature region) can also be derived [13] from equation (1*a*). Therefore, the small-polaron hopping model and the VRH model might be applicable for many semiconducting systems.

Among the many rare-earth manganates already studied, the $La_{1-x}Pb_xMnO_3$ system is an interesting one as this system showed giant magnetoresistance around room temperature [14]. Recently, Ji *et al* [15] also studied the transport and electron paramagnetic resonance in $La_{0.6}Pb_{0.4}MnO_3$ and it was suggested that both double-exchange and electron–phonon coupling are responsible for the giant magnetoresistance around the semiconductor-to-metallic transition (SMT) temperature. The thermoelectric power of the Pb-doped sample has also been reported by Mandal [16]. However, we believe the mechanisms of electrical transport in this and similar other magnetic semiconductors, in the high-temperature region (above SMT), have not been clearly understood. Particularly, the contribution of the polarons in the transport mechanism has not been well elucidated in these oxides showing SMT. Recently, Viret *et al* [13] reported non-adiabatic hopping and Chatterjee *et al* [17] reported both adiabatic and non-adiabatic hopping mechanisms (depending on concentration) in such rare-earth manganates. Above the SMT temperature, some groups reported semiconducting behaviour $\ln(\rho/\rho_\infty) = E_a/kT$ [18] with activation energy of the order of 0.2 eV, while others find their conductivity data (above SMT) can be fitted well by Mott's VRH model [5, 13, 19–21] which is actually valid in the low temperature region (<100 K). It has also been pointed out earlier [22–24] that much of the behaviour of resistivity above the magnetic transition is indicative of conduction by magnetic polarons. But the real picture of the polaron hopping conduction mechanism in the high temperature region seems to be more complicated. For better understanding of the situation, conductivity data need to be thoroughly examined and fitted with the possible hopping models proposed by Mott [12], Schnakenberg [25] and Emin and Holstein [11, 26] confirming the polaronic conduction, which has been done in this paper. Like electrical conductivity, the thermoelectric power (TEP) of these oxides is also interesting [3, 5] showing giant thermoelectric power and its magnetic field dependence around the SMT temperature.

In the present paper we report the concentration (x) -dependent electrical resistivity (in the presence or in the absence of a magnetic field) and TEP of the $La_{1-x}Pb_xMnO_{3+\delta}$ system (with $x = 0-0.5$) in the temperature range 330–80 K. It is observed, in contrast to some earlier observations by different authors, that two kinds of hopping mechanism (adiabatic and non-adiabatic) are followed by $LaMnO_3$ (for $x = 0$ showing no SMT) and $La_{1-x}Pb_xMnO_3$ (for $x > 0$ showing SMT) in the high temperature regime ($T > \theta_D/2$). Here we should emphasize that the measurements reported here were on sintered samples, rather than melt-grown single crystals. Such measurements are always potentially affected by intergranular effects. Although, therefore, not totally unambiguous, we will argue that the main finding of this is the behaviour of hopping conduction mechanism on the bulk material and not the intergranular contacts. Even hopping between the micrograins is a possible conduction mechanism in disordered materials [27]. For many bulk granular semiconductors like $LaFe_xNi_{1-x}O_3$ [28], La_2CuO_4 [29], $La_{1-x}Sr_{1+x}FeO_4$ [28], etc the small-polaron hopping model and the VRH model have been successfully used.

2. Experimental details

All the $La_{1-x}Pb_xMnO_{3+\delta}$ ($x = 0$, 0.05, 0.1 and 0.5) samples were prepared by a solid-state reaction technique similar to our earlier work [30, 31] using appropriate amounts of La_2O_3, $MnCO_3$ and PbO, each of purity 99.99%. The x-ray structural study was made with a diffractometer (model: Seifert X-Dal-3000). For each of the samples, the value of the ratio $C = 1/(1 + z)$ where $z = Mn^{4+}/Mn^{3+}$ was determined in a non-destructive way from the magnetic susceptibility and density data (these values of C agree quite well within $\pm 5\%$ with those measured by chemical means). Atomic absorption studies indicated about 1–2 wt% loss of Pb compared to the initial composition of the raw materials used. This is mainly due to the evaporation loss of PbO that occurred during high temperature annealing of the samples in air. The electrical resistivity and TEP of the samples were measured between 330 and 80 K using an APD cryo-cooler unit with a temperature controller following the procedure reported earlier [32] with an accuracy better than $\pm 2\%$. Magnetoresistances of the samples were measured between room temperature and 80 K in a magnetic field of 1.5 T (maximum). Resistivity of two samples with the same concentration (x) prepared under similar conditions was found to vary within $\pm 1\%$. Magnetic susceptibilities (paramagnetic above the SMT temperature) of all the samples were measured by VSM above the SM transition temperature. The x-ray diffraction patterns of the undoped $LaMnO_3$ sample indicated an orthorhombic structure in agreement with that obtained by Mahendiran *et al* [1]. Structural analysis of the oxide sample indicated rhombohedral structure below $x = 0.5$ and cubic structure above $x = 0.5$. For the $x = 0.3$ composition, the rhombohedral lattice parameter is found to be $a \sim 5.388$ Å with rhombohedral angle $\sim 61.55^\circ$. For the cubic ($x = 0.5$) sample, the lattice constant $a \sim 7.88$ Å, which is comparable with those estimated by Mahendiran *et al* [14] and Ji *et al* [15].

3. Results and discussion

3.1. High temperature ($T > \theta_D/2$) hopping conduction

Figure 1 represents the thermal variation of resistivity of $La_{1-x}Pb_xMnO_3$ with $x = 0.0$ (figure 1(a) showing no SMT), and $x = 0.05$, 0.1 and 0.5 (figure 1(b) showing SMT) in the absence and in the presence of a magnetic field (maximum field 1.5 T). All the Pb-doped $La_{1-x}Pb_xMnO_3$ samples underwent metal–insulator transitions showing peak temperatures (T_p) between 230 and 275 K (table 1). Negative magnetoresistance

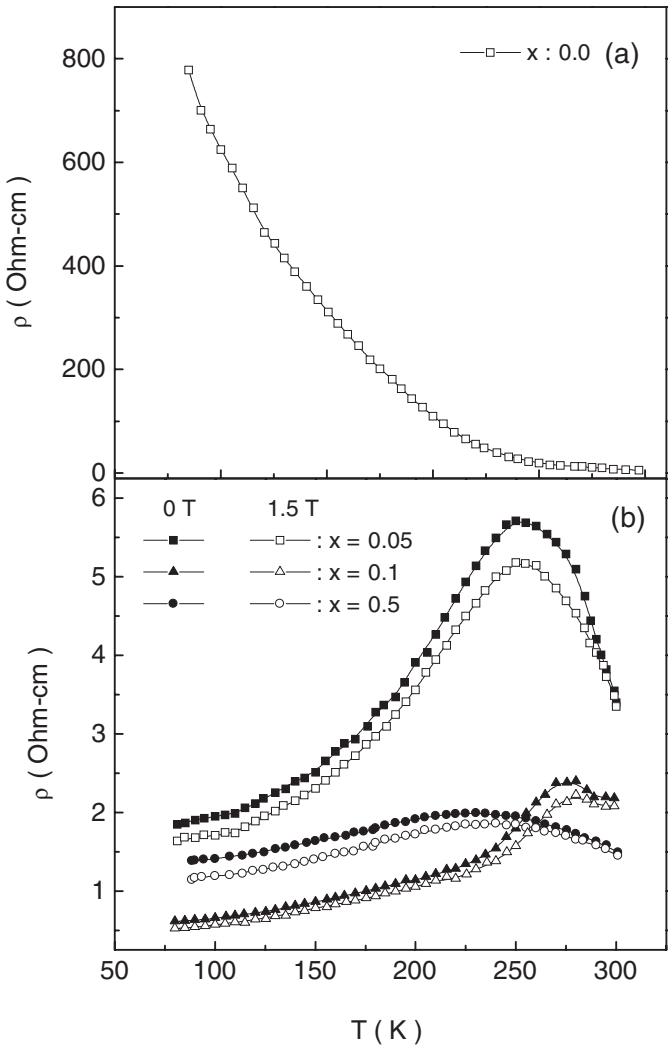

Figure 1. Thermal variation of resistivity (ρ) of $La_{1-x}Pb_xMnO_3$ samples with (a) $x = 0.0$ at zero magnetic field and (b) $x = 0.05$, 0.1 and 0.5 at zero and 1.5 T magnetic field. Solid lines are guides for the eyes.

is observed, as usual, for all the Pb-doped samples of our present investigation as shown in figure 2 for a typical sample $La_{0.9}Pb_{0.1}MnO_3$. In figure 3, the non-linear variation of $\log \sigma_{dc}$ versus inverse temperature curve (for $T > T_p$) indicates temperature-dependent activation energy, which is a characteristic of small-polaron hopping conduction [33, 34]. Such a consistent thermal behaviour of the undoped and Pb-doped semiconductors (above SMT) cannot be explained by the grain boundary effect, which is primarily effective in the low temperature metallic regime [35]. Therefore, the polaron hopping conduction mechanism appears to be applicable in the high temperature ($T > T_p$) region (as discussed below in detail). As the temperature is increased above T_p, there is a deviation from linearity (figure 3). The temperature at which the slope in the high temperature range changes from linearity is considered to be $\theta_D/2$ (where θ_D is

Table 1. Some important parameters of the $La_{1-x}Pb_xMnO_3$ system showing metal–insulator transitions (values within the brackets indicate maximum errors).

x	T_p (K)	C	Density (gm cm^{-3})	W (eV)	θ_D (K)	γ_{ph} ($=k_B\theta_D/h$) ($\times 10^{-13}$ Hz)	N (cm^{-3})
0.0		0.89 (±0.05)	4.016 (±0.005)	0.150	470 .59 (±2.0)	0.981	5.15×10^{21}
0.05	252.5 (±0.5)	0.88 (±0.05)	4.054 (±0.005)	0.132	563.38 (±2.0)	1.166	7.29×10^{21}
0.1	275.0 (±0.5)	0.83 (±0.05)	4.095 (±0.005)	0.056	564.97 (±2.0)	1.169	5.34×10^{21}
0.5	230.0 (±0.5)	0.59 (±0.05)	5.669 (±0.005)	0.013	527.71 (±2.0)	1.092	9.43×10^{21}

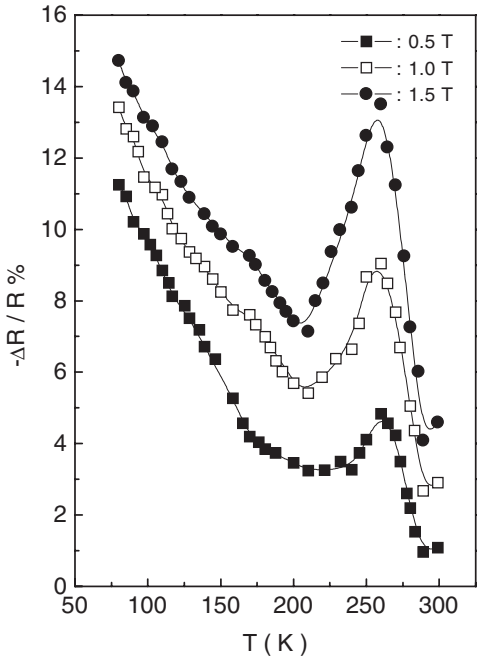

Figure 2. Thermal variation of magnetoresistance of a typical sample $La_{0.9}Pb_{0.1}MnO_3$ at different magnetic fields showing negative magnetoresistance. Solid lines are guides for the eyes.

the characteristic Debye temperature) [12]. The linear semiconducting part of the samples (for $T > \theta_D/2$) is well explained by Mott's small-polaron hopping model [12] (equation (1*b*)). The expression for the high temperature ($T > \theta_D/2$) dc conductivity (σ_{dc}) as given by Mott can be written as

$$\sigma_{dc} = \sigma_0[\exp(-W/k_BT)]. \tag{1b}$$

A similar equation was also used earlier [1, 5, 6, 17] to fit the conductivity data of rare-earth manganates or other mixed-valence granular semiconducting oxides such as $LaFe_xNi_{1-x}O_3$ [28], $La_{1-x}Sr_x(Mn,Co)O_3$ [36], etc with W as the activation energy. According to the small-polaron hopping model of Mott [12], $\sigma_0 = [\nu_{ph}Ne^2R^2C(1-C)]\exp(-2R\alpha)/k_BT$, k_B is

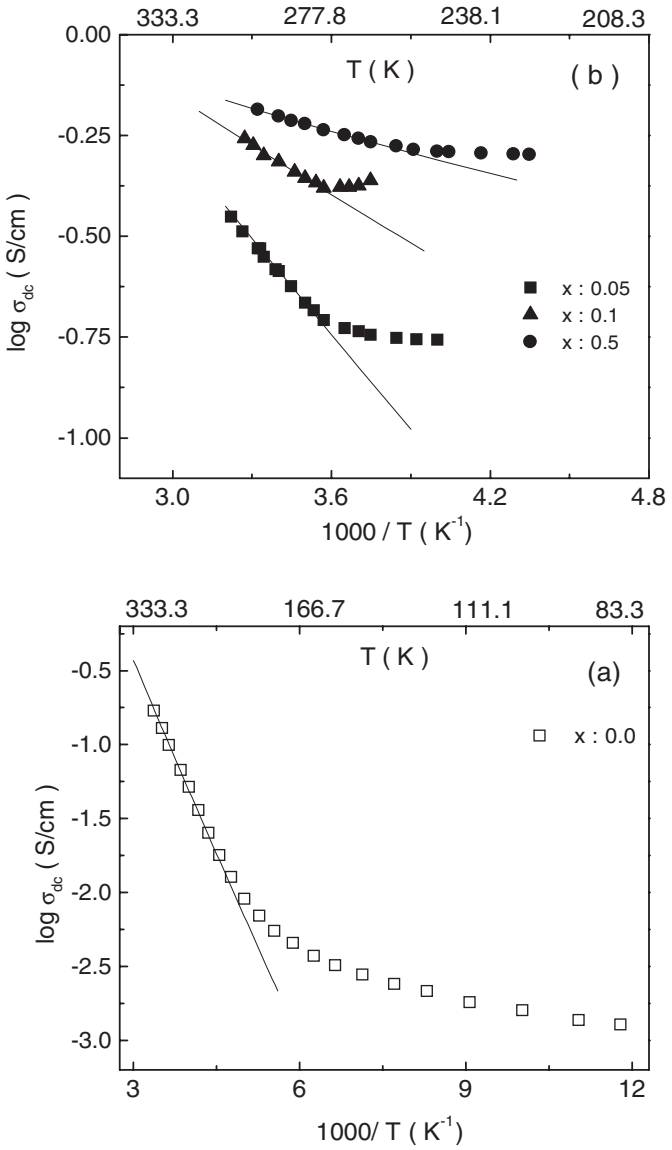

Figure 3. Variation of $\log \sigma_{dc}$ as a function of inverse temperature $1000/T$ above the respective SMT temperature T_p for (a) $LaMnO_3$ and (b) $La_{1-x}Pb_xMnO_3$ with $x = 0.05$, 0.1 and 0.5 (shown for $T > T_p$). The solid lines give the best fit to Mott's equation (1) at higher temperatures ($T > \theta_D/2$).

the Boltzmann constant and T is the absolute temperature. N, ν_{ph}, α and R are, respectively, the number of transition metal (Mn) ions per unit volume (obtained from the density data as shown in table 1), the phonon frequency, tunnelling probability and average hopping distance (Mn–O–Mn). The ion–ion separation greatly influences the conduction mechanism [18]. When the overlap integral $J_0 \exp(-2R\alpha)$ approaches J_0, the hopping is adiabatic ($\alpha \sim 0$) and the semiconducting behaviour is then controlled mainly by the activation energy. Hence $\sigma_{dc} \sim \sigma_0 \exp(-W/k_B T)$, otherwise the hopping conduction mechanism is non-adiabatic

($\alpha \neq 0$). Equation (1*b*) can explain the semiconducting behaviour of all the samples in the high temperature range ($T > \theta_D/2$). The values of W and θ_D (table 1) for the present samples estimated from the experimental conductivity data (figure 3) are used to fit equation (1*b*). The activation energy W, which is found to be larger for the undoped $LaMnO_3$ sample (table 1) and decreases with increasing Pb concentration, plays an important role in the conduction mechanism in this high temperature region. For the undoped $LaMnO_3$, the Debye temperature (θ_D) is smaller (table 1) than those of the Pb-doped samples. The activation energy (W) for the hopping conduction can be written as [34], $W = W_H + W_D/2$ (for $T > \theta_D/2$) and $W = W_D$ (for $T < \theta_D/4$), where W_H is the polaron hopping energy, W_D is the disorder energy (can be estimated independently from the Schnakenberg model [25] discussed below). The hopping energy W_H is calculated from the relation [12]

$$W_H = \frac{e^2}{4\varepsilon_p}(1/r_p - 1/R) \tag{2}$$

where $\varepsilon_p = (1/\varepsilon_s - 1/\varepsilon_\infty)$. ε_∞ and ε_s are the high frequency and static dielectric constants of the samples. The values of ε_p obtained from the dielectric constant data (unpublished) of the Pb-doped and undoped samples vary from 5 to 20 (shown in table 2) and they are almost constant within the semiconducting temperature range between T_p and 330 K of our measurements. The polaron radius r_p is estimated [37] from the knowledge of N (table 1) using the relation $r_p = (1/2)[\pi/6N]^{1/3}$. In the present Pb-doped system, r_p (table 2) is found to vary between 1.90 and 2.33 Å (depending on the Pb concentration), which is much smaller than R (varying between ~4 and 5 Å as shown in table 2). This apparently suggests that the polarons are indeed small polarons and they are localized in the Mn sites. The values of W_H calculated from equation (2) (using r_p and ε_p from table 2) are also given in table 2. For the stoichiometric $LaMnO_3$ system with larger r_p value, compared to the corresponding Pb-doped samples, no SMT transition was observed. A good fit (solid line in figure 3) to the high temperature ($T > \theta_D/2$) experimental conductivity data of all the samples (doped and undoped) with equation (1) indicates that the conduction of charge carriers is mainly governed by the small-polaron hopping mechanism. Recently, transport measurements on $La_{1-x}Ca_xMnO_{3+\delta}$ oxides by Hundley *et al* [6] have also confirmed the adiabatic small-polaron hopping mechanism in these type of oxides which supports our finding. In fact, the small-polaron transport mechanism was also applied by Wang *et al* [24] to explain dc conductivity of Zn-doped $Fe_{1-x}Zn_xCr_2S_4$ system showing colossal magnetoresistance. Although earlier, the entire experimental dc conductivity data above SMT temperature were fitted [5, 13, 19] with the VRH model, it is considered to be neither strictly realistic nor necessary. It is found that the high temperature data (for $T > \theta_D/2$) of all the samples are well fitted

Table 2. Activation energy (W), hopping energy (W_H), dielectric constant (ε_p)[a], polaron band width J and other fitting parameters obtained from fitting the DC conductivity data of $La_{1-x}Pb_xMnO_3$ ($x = 0.0, 0.05, 0.1$ and 0.5) oxides with different theoretical equations as discussed in the text.

x	W_H (eV) (from equation (2))	r_p (Å)	R (Å)	ε_p	J (eV)
0.0	0.184	2.334	5.792	4.85 ± 0.02	0.021
0.05	0.052	2.077	5.155	5.75 ± 0.02	0.084
0.1	0.049	2.306	5.723	11.51 ± 0.02	0.096
0.5	0.196	1.908	4.733	18.49 ± 0.02	0.211

[a] Measured by the impedance analyser (HP Model 4192).

with equation (1). Similarly, the corresponding low temperature data (for $T < \theta_D/2$) can also be fitted well with the VRH model (as discussed below). As mentioned above, equation (1*b*) fits the high temperature (above $T > \theta_D/2$) conductivity (σ_{dc}) data of $LaMnO_3$ with $\alpha = 2.5\ nm^{-1}$ (using the values of R from table 1). The non-zero value of α and hence $\exp(2\alpha R)$ indicates that in this high temperature region the non-adiabatic hopping conduction mechanism is followed by this sample. On the other hand, the corresponding high temperature σ_{dc} data of all the Pb-doped samples showing SMT fit equation (1), with $\exp(2\alpha R) = 1$ (or $\alpha = 0$), which indicates that above $T > \theta_D/2$ the adiabatic hopping conduction mechanism is valid for these Pb-doped samples showing SMT. The theoretical fitting curves are shown by the continuous lines in figures 3(a) and (b) (high temperature $T > \theta_D/2$ part only). Here it should be mentioned that it is rather difficult to uniquely identify the type of small-polaron hopping conduction mechanism, adiabatic or non-adiabatic, if only the temperature dependence of conductivity is used, because the conductivity subject to the adiabatic small-polaron conduction also satisfies the temperature dependence of non-adiabatic hopping conduction [38, 39]. So other supporting methods are to be used to confirm the nature of hopping conduction in this system (to be discussed). Before doing this, we first attempt to apply the VRH model to fit the low temperature ($T < \theta_D/2$) conductivity data of the samples.

3.2. Low temperature ($T < \theta_D/2$) VRH model

In the three-dimensional cases, conductivity following the VRH mechanism is predicted from the following relation [12, 33]:

$$\sigma_{dc} = \sigma_0 \exp\left[-(T_0/T)^{1/4}\right] \tag{3}$$

where T_0 is a constant [$=16\,\alpha^3/k_B\,N(E_F)$] and $N(E_F)$ is the density of states at the Fermi level, which can be calculated from the slope of the plot of $\log\sigma_{dc}$ versus $T^{-1/4}$ curves (shown in figures 4(a) and (b), for all the samples. Interestingly, it is observed from figure 4 that the temperature-dependent conductivity of semiconducting $LaMnO_3$ without showing SMT can be divided into three linear regions (low, intermediate and high temperature regions). This indicates a change of conduction mechanism with change of temperature. The corresponding change of slope of the curves of the Pb-doped samples above SMT, however, showed only two such linear regions (high and low temperature parts above the SMT temperature). The best fit to the low temperature data (solid line below $\theta_D/2$ in figure 4(a)) of $LaMnO_3$ occurs with $T_0 \sim 10^6$ K and $\chi^2 \sim 2.71$–2.83 (for different slopes, where χ^2 is the weighted sum of the squared deviations). The values of $N(E_F)$ obtained for the two low temperature slopes of $LaMnO_3$ are, respectively, 3.348×10^{20} and $2.076 \times 10^{22}\ eV^{-1}\ cm^{-3}$. These values of $N(E_F)$ are higher than those of the usual oxide semiconductors which vary from 10^{17} to $10^{19}\ eV^{-1}\ cm^{-3}$. For the estimation of $N(E_F)$, we used as before $\alpha = 2.5\ nm^{-1}$ obtained from fitting the conductivity data with equation (1). For the Pb-doped samples, as mentioned above, there is only one slope for each of the samples below $\theta_D/2$ where the VRH model is found applicable. The solid lines (below $\theta_D/2$) in figures 4(b) and (c) indicate the best-fit curve with equation (3). Using the same value of $\alpha = 2.5\ nm^{-1}$, the values of $N(E_F)$ were also calculated for all the Pb-doped samples. These values of $N(E_F)$ are found to be of the order of 10^{21} and $10^{22}\ eV^{-1}\ cm^{-3}$. Such a high value of $N(E_F)$ also indicates adiabatic hopping conduction in the low temperature region, which will be clear from the subsequent discussion. Here we should mention that using the VRH model Viret *et al* [13] also estimated $\alpha = 2.22\ nm^{-1}$ for the La–Sr–Mn–O system showing SMT. The values of $N(E_F)$ estimated for the present Pb-doped samples also agree with that ($\sim 10^{22}\ eV^{-1}\ cm^{-3}$) estimated by Viret *et al* [13]. It is noted

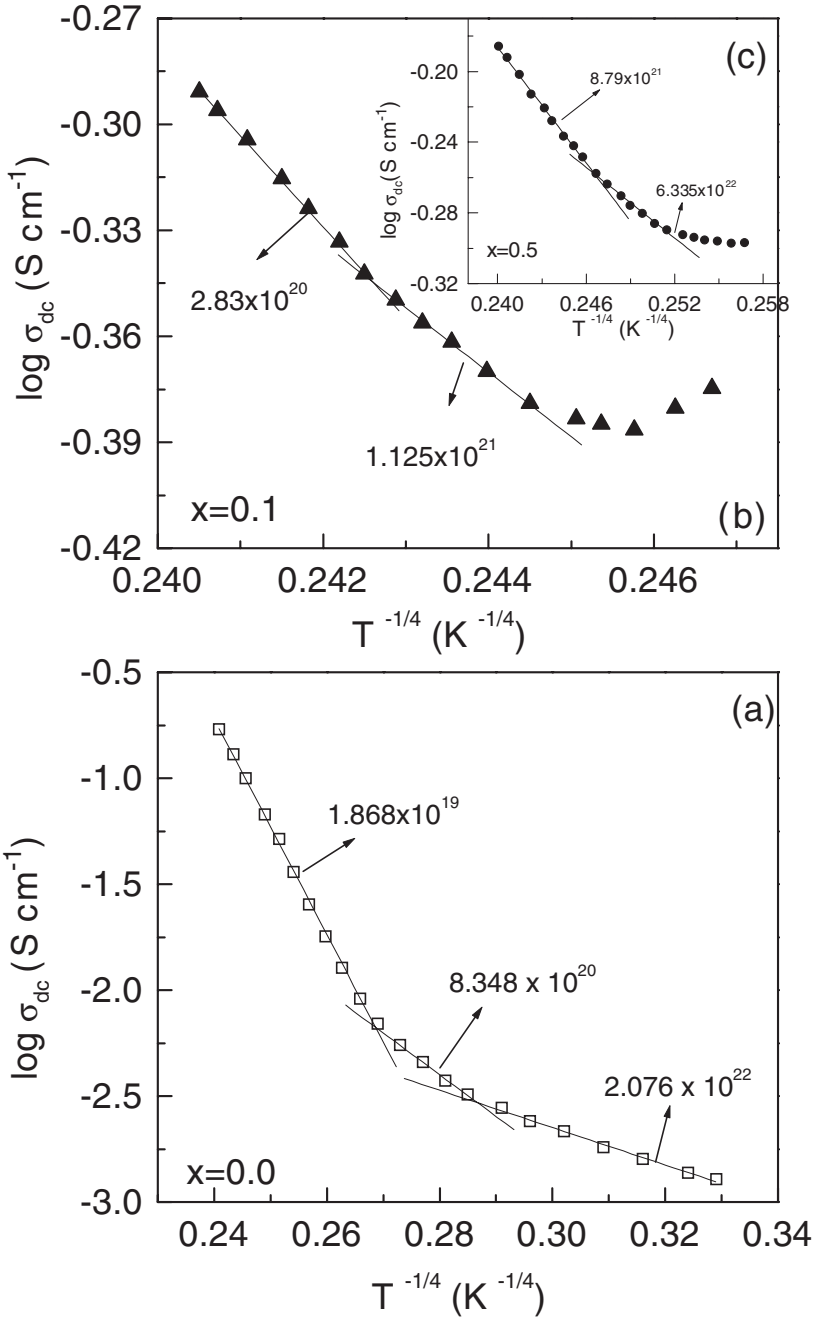

Figure 4. Variation of $\log \sigma_{dc}$ as a function of $T^{-1/4}$ above the respective SMT temperature T_p for (a) $LaMnO_3$ showing three linear regions (low, intermediate and high temperature parts) and (b) $La_{1-x}Pb_xMnO_3$ with $x = 0.1$ and 0.5 (showing low and high temperature parts). Solid lines are the best fit theoretical curves with the VRH model (equation (3)). Values against each straight line (slope) in the curve indicate $N(E_F)$ in units of eV^{-1} cm^{-3}.

that the low temperature values of $N(E_F)$ of the Pb-doped samples showing SMT are similar in magnitude to the corresponding low temperature values of the undoped $LaMnO_3$ sample (shown in figure 4(a)). Thus it is clear that the VRH model is valid for all the samples in the low temperature region ($<\theta_D/2$) with higher values of $N(E_F)$ compared to those of the usual semiconducting samples. This is because of the higher conductivity of the present samples from that of the usual oxide semiconductor following the small-polaron hopping mechanism.

3.3. VRH model at high temperature

Transport properties in many mixed-valence polycrystalline semiconducting oxides like $LaFe_xNi_{1-x}O_3$ [22], $LaCuO_4$ [29], etc have been described by VRH of charge carriers. But the temperature range over which the hopping model is satisfied is found to be different for different materials. Recently, Jaime *et al* [5], Viret *et al* [13] and Crespi *et al* [19] also applied the VRH conduction mechanism, respectively, for similar types of samples, namely $Nd_{1-x}(Sr, Pb)_xMnO_3$, $La_{0.8}Ca_{0.2}MnO_3$, for the entire range of temperature above SMT, i.e. above 200 K. But it has already been shown above that the VRH model (equation (3)) well fits the low temperature conductivity data of all the samples and one need not fit the high temperature data with the VRH model. The validity of the VRH model for the present system for such a high temperature range ($>T_p$) should, therefore, be clarified. It has been shown [40] that depending on the strength of the Coulomb interaction, the expression for the density of states at the Fermi level is modified and the VRH model may be applied even at higher temperature ($\sim$300 K and above). In the following paragraph we have shown that the VRH model may also be used for fitting the high temperature ($T > \theta_D/2$) conductivity data, though this fitting gives no new result and seems to be unnecessary.

It is seen from figure 4(a) that the high temperature (>180 K) conductivity data of the insulating $LaMnO_3$ sample can be described by a single straight line following the three-dimensional VRH model (equation (3)). Similarly, for the Pb-doped samples showing SMT, the three-dimensional VRH model is also applicable above $\theta_D/2$. But the entire temperature range of the curve (above SMT) for any of the samples (doped or undoped), cannot be fitted with the same model parameters (being different for different samples) as the slope of the curve changes with temperature (figure 4). This is in contrast to the reported results [5, 13, 19] where the VRH model was used to fit the data above SMT. From this high temperature fitting of the conductivity data with equation (3), an estimation of $N(E_F)$ has also been made. For the undoped $LaMnO_3$, using the same value of $\alpha = 2.5\ nm^{-1}$, we have $N(E_F) \sim 1.8 \times 10^{19}\ eV^{-1}\ cm^{-3}$ (from equation (3)) which is, interestingly, comparable to those of many semiconducting transition metal oxides [41]. It has been shown below that this value of $N(E_F)$ also suggests non-adiabatic hopping conduction in $LaMnO_3$ in the high temperature region as that obtained from equation (1b). The high temperature conductivity data of the Pb-doped samples are fitted with equation (3) as shown by the solid line in figures 4(b) and (c). To estimate $N(E_F)$ for these Pb-doped samples in the high temperature range, the same value of $\alpha \sim 2.5\ nm^{-1}$ is again used which yields $N(E_F) \sim 10^{20}-10^{21}\ eV^{-1}\ cm^{-3}$, depending on Pb concentrations (figure 4). It has already been mentioned that Viret *et al* [13] also estimated similar values of α and $N(E_F)$ for the manganate samples. Thus, from fitting of the high temperature conductivity data ($>\theta_D/2$) with the VRH model, the value of $N(E_F)$ for the present Pb-doped sample showing SMT comes out to be more than two orders of magnitude higher than that of $LaMnO_3$ showing no SMT. Such a high value of $N(E_F)$ for the Pb-doped samples also indicates an adiabatic hopping conduction mechanism (discussed below) in the high temperature region ($T > \theta_D/2$) supporting the result obtained from equation (1).

3.4. Nature of hopping conduction

We have now three sets of values of $N(E_F)$ estimated for $LaMnO_3$ for three different temperature ranges (high, intermediate and low as shown in figure 4(a)) and two sets of corresponding values for the Pb-doped samples in the two temperature ranges (high and low as shown in figure 4(b) and (c)). Knowing these values of $N(E_F)$ one can find the nature of the hopping conduction and how the hopping mechanism changes in the samples from Holstein's condition [11]. According to this condition, the polaron bandwidth J should satisfy the inequality $J > \phi$ (for adiabatic hopping conduction) and $J < \phi$ (for non-adiabatic hopping conduction) where

$$\phi = (2k_B T W_H/\pi)^{1/4}(h\nu_{ph}/\pi)^{1/2}. \tag{4}$$

Using the values of W_H from table 1, the values of ϕ are calculated from the right hand of equation (4) as shown in table 3 (for the high temperature region of conductivity data). The values of J are also calculated independently from the model proposed by Mott and Davis [12], namely $J \sim e^3[N(E_F)/\varepsilon_p^3]^{1/2}$. Taking the values of $N(E_F)$ and ε_p from tables 2 and 3, the estimated J values are also listed in table 3. Now comparing these J values with those of ϕ, it is observed that only for the $LaMnO_3$ system without SMT, is $J < \phi$ (non-adiabatic hopping condition) strictly satisfied in the high temperature ($T > \theta_D/2$) range. But in the low and intermediate temperature range with large values of $N(E_F)$, $LaMnO_3$ also follows the adiabatic hopping mechanism. Thus, in the undoped $LaMnO_3$ sample we notice a change of conduction mechanism from non-adiabatic (high temperature range) to adiabatic (low and intermediate temperature ranges). On the other hand, for all the doped samples showing SMT, the adiabatic hopping condition ($J > \phi$) is satisfied throughout the range of temperature (high and low). This is in agreement with our earlier observation from fitting of the conductivity data of the samples with equation (1). Thus, a change-over from the non-adiabatic to the adiabatic hopping conduction mechanism occurs with Pb doping in the $LaMnO_3$ samples (or with increase of Mn^{4+} concentration in the rare-earth manganates). It is to be noted that the $N(E_F)$ value of $LaMnO_3$ increases as the temperature decreases and in the low temperature region ($T < \theta_D/2$), the $N(E_F)$ value of this sample is almost equal in magnitude with those of the low temperature values of the Pb-doped samples.

Table 3. Different parameters obtained by fitting DC conductvity data of the $La_{1-x}Pb_xMnO_3$ system with different theoretical models discussed in the text. W_H and W_D are obtained from fitting with Schnakenberg's model (equation (5)).

x	W_H (eV)	W_D (eV)	J (eV)	ϕ (eV)	$N(E_F)$ (eV^{-1} cm^{-3}) ($\alpha = 0.25$ $Å^{-1}$) for $T > \theta_D/2$
0.0	0.190	0.090	0.022	0.026	1.868×10^{19}
0.1	0.081	0.051	0.024	0.023	2.830×10^{20}
0.5	0.061	0.020	0.065	0.021	8.790×10^{21}

Another test of the adiabatic hopping conduction in the present La–Pb–Mn–O system (for $T > \theta_D/2$) is made from the independent calculations of the hopping energy W_H from the theory of Schnakenberg [25] who showed that in the scenario of $T > \theta_D/2$, the main contribution to σ_{dc} above the metal–insulator transition (insulating phase) comes from the phonon-assisted conductivity. The high temperature conductivity in this model is given by

$$\sigma_{dc} = \sigma_0 T^{-1}[\sinh(h\nu_{ph}\beta)]^{1/2}\exp[-(4W_H/h\nu_{ph})[\tanh(h\nu_{ph}\beta/4)]\exp[-W_D\beta]. \tag{5}$$

The experimental conductivity data of all the samples have also been fitted to the Schnakenberg model [25] (equation (5)) and the best-fit parameters, W_H and W_D, are listed in table 3. The

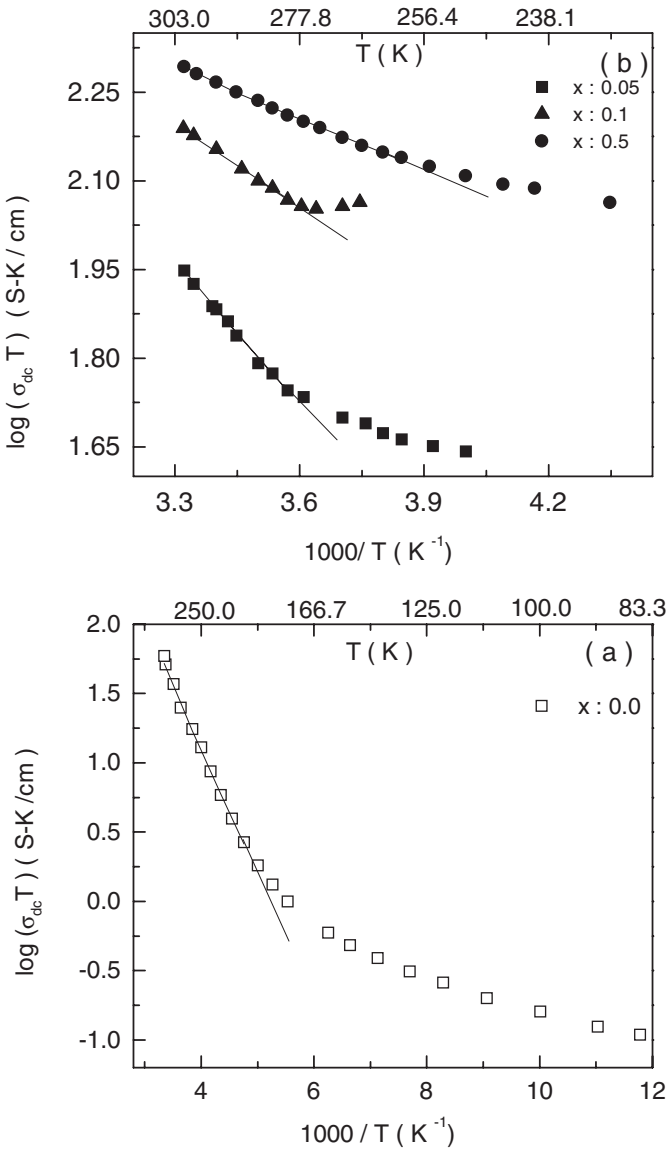

Figure 5. Plot of $\log(\sigma_{dc}T)$ versus $1000/T$ for (a) $La_{1-x}Pb_xMnO_3$ system above SMT and $\theta_D/2$ with $x = 0$ and (b) $x = 0.05$, 0.1 and 0.5. The solid line corresponds to the best fit with Schnakenberg's model (equation (5)).

same values of phonon frequency shown in table 1 were used in this fitting. The values of W_H and W_D are consistent with those of semiconducting oxides. In figure 5, $\log(\sigma_{dc}T)$ has been plotted as a function of $1000/T$ for the undoped ($x = 0$) and doped samples ($x = 0.05$, 0.1 and 0.5), for high temperature $T > \theta_D/2$ only. The theoretical best-fit curve is shown by the straight line. Using these values of W_H, ϕ is estimated (from equation (4)), which is found to vary from 0.024 to 0.0188 eV for the Pb-doped $La_{1-x}Pb_xMnO_3$ system ($x = 0.1$–0.5), and hence smaller than the corresponding J values of the samples shown in

table 3. Again, the adiabatic hopping conduction mechanism is confirmed valid for the Pb-doped samples showing metal–insulator transition transitions. On the other hand, for the undoped $LaMnO_3$, the corresponding estimated value of ϕ is $\sim$0.037 eV, which is larger than the J value ($\sim$0.021 eV shown in table 3) and hence supports non-adiabatic hopping conduction in $LaMnO_3$ showing no SMT (for $T > \theta_D/2$).

Non-adiabatic small-polaron hopping conduction in the undoped $LaMnO_3$ oxide is also supported from the small-polaron hopping model proposed by Emin and Holstein [11]. It may be noted that a small polaron is formed when the electron–phonon interaction is strong enough [11]. Following Holstein [11], Gorham-Bergeron and Emin [42], the dc conductivity for the non-adiabatic hopping of small polarons in the high temperature range ($T > \theta_D/2$) can be written as

$$\sigma_{dc} = (Ne^2R^2/6k_BT)(J/h)^2\left[(\pi/h^2)/2\left(E_c^{op}+E_c^{ac}\right)k_BT\right]^{1/2}\exp\left[W_D^2/8\left(E_c^{op}+E_c^{ac}\right)k_BT\right] \times \exp[-W_D/2k_BT]\exp\left[-E_A^{op}/k_BT - E_A^{ac}/k_BT\right] \quad (6)$$

where

$$E_c^{op} = E_b^{op}(1/N_p)\sum[h\nu_{o,q}/2k_BT]\,\mathrm{cosech}(h\nu_{o,q}/2k_BT)$$
$$E_c^{ac} = E_b^{ac}(1/N_p)\sum[h\nu_{a,q}/2k_BT]\,\mathrm{cosech}(h\nu_{a,q}/2k_BT)$$
$$E_A^{op} = E_b^{op}(1/N_p)\sum[h\nu_{o,q}/2k_BT]\tanh(h\nu_{o,q}/2k_BT)$$
$$E_A^{ac} = E_b^{ac}(1/N_p)\sum[h\nu_{a,q}/2k_BT]\tanh(h\nu_{a,q}/2k_BT).$$

$\nu_{o,q}$ and $\nu_{a,q}$ are the optical and acoustical phonon frequencies, respectively, at wave vector q. N_p is the number of phonon modes, E_b^{op} and E_b^{ac} are the polaron binding energies related to optical and acoustical phonons, respectively. Equation (6) has been utilized in calculating the non-adiabatic dc conductivity of the $LaMnO_3$ system, assuming that the acoustic phonon density of states is approximately given by $g(\omega) \propto \omega^2$ and that the mean optical phonon frequency, ν_{ph}, is constant. Using the value of W_D, from table 3, the high temperature conductivity data of the undoped $LaMnO_3$ can be fitted to equation (6) with parameters $E_c^{ac}(\mathrm{eV})\times10^2 = 3.9$, $E_c^{op}(\mathrm{eV})\times10^2 = 3.9$, $E_a^{ac}(\mathrm{eV})\times10^2 = 7.50$ and $E_a^{ac}(\mathrm{eV})\times10^2 = 7.50$. This again supports the non-adiabatic hopping conduction mechanism as valid for this sample. Similar calculations can also be extended to show the adiabatic hopping conduction mechanism followed by the corresponding Pb-doped system.

3.5. Thermoelectric power

The SMT is also well reflected from the thermoelectric power measurements since the contribution of the carriers to the TEP depends directly on the fractional concentration of holes/electrons in polaronic system [5, 6, 19]. Figure 6(a) shows the temperature variation of TEP between 300 and 80 K of a typical $La_{1-x}Pb_xMnO_3$ system with $x = 0.1$ exhibiting metal–insulator transitions. Detailed discussion on the concentration (Pb)-dependent TEP of these Pb-doped samples has recently been reported by Mandal [16]. He, however, did not report the TEP data of the sample with $x = 0.1$ and the magnetic field dependence of thermopower. Polaron hopping conduction is also supported from the temperature-dependent Seebeck coefficient data. According to the small-polaron theory [6, 43, 44], the Seebeck coefficient can also be written as

$$S(T) = (k_B/e)[\eta_e + W_e/k_BT] \quad (7)$$

where η_e is a sample-dependent constant and W_e is the energy difference between identical lattice distortion. The thermal variation of TEP data of the sample both in the presence and

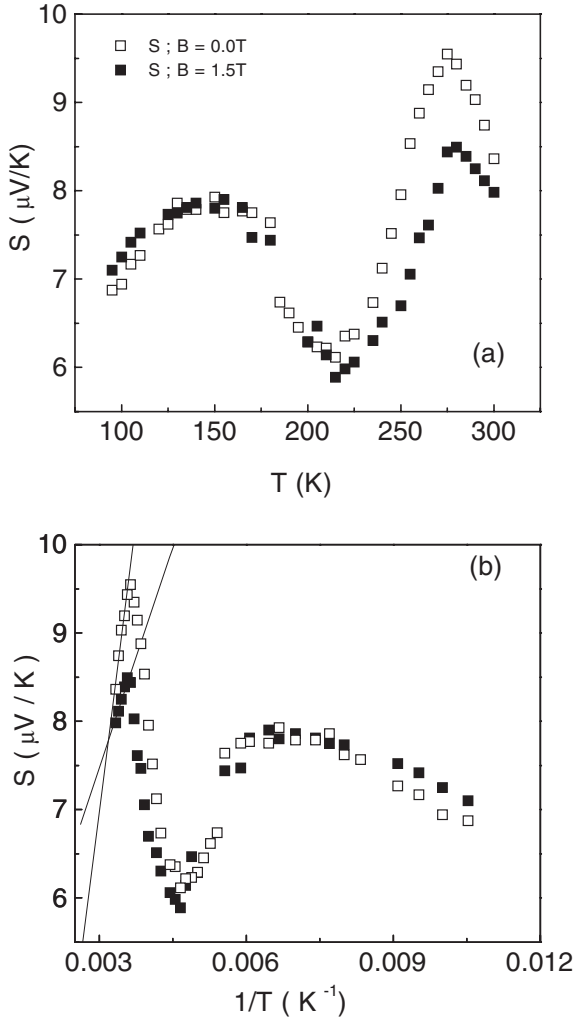

Figure 6. Variation of thermopower $S(T)$ of $La_{1-x}Pb_xMnO_3$ (with $x = 0.1$) as a function of temperature (a) and as a function of inverse temperature (b) both in the presence and the absence of a magnetic field. Appreciable field dependence is observed around the SMT temperature.

absence of a magnetic field is shown in figure 6(a) exhibiting a giant peak around the SMT temperature. The linear part of the TEP data of this curve (solid line in figure 6(b)) above SMT was fitted with equation (7). The observed significant difference (also observed by others [3, 5, 19]) between the activation energy obtained from the conductivity data ($W = 56$ meV) and TEP data ($W_s = 4.36$ meV) is a characteristic of the small polaron [3, 5, 19, 44, 45]. Very little work has been done on the magnetic field dependent thermoelectric power [45]. Field dependence of TEP data indicates local ordering of the magnetic moments around the SMT transition region (fluctuating region) as shown in figure 6(a). The field dependence of the Seebeck coefficient, which is quite large around SMT (figure 6(a)), is an indication of the importance of spin-ordering and its contribution to the transport mechanism, which has not been well analysed. We also estimated the field dependence of W_s ($W_s = 1.7$ meV) for this

sample, which is smaller than the corresponding field independent value ($W_s = 4.36$ meV). It is also noted (not discussed in this paper) that the low temperature conductivity data (below SMT) in the metallic region (linear part of the curve in figures 1(b) and 2) can be fitted with an equation of the form $\rho(T < T_p) = \rho_0 + T^{2.5}$, where ρ_0 is the temperature-independent resistivity due to grain boundary and the presence of the temperature-dependent part indicates the importance of electron–magnon interaction [46].

4. Conclusion

In conclusion, temperature-dependent (330–80 K) electrical conductivity and thermopower (TEP) measurements of the Pb-doped $La_{1-x}Pb_xMnO_3$ ($x = 0.1$–0.5) system have revealed metal–insulator transitions between 230 and 275 K. The high temperature conductivity data can be successfully fitted with the polaron-hopping conduction theory like that of usual oxide semiconductors. Interesting changes in the conduction mechanism have been observed in the temperature range between SMT and 330 K. For the undoped $LaMnO_3$ system ($x = 0$), this temperature range can be divided into three parts (high, intermediate and low) while for the doped samples there are only high and low temperature parts. The $LaMnO_3$ sample without showing SMT is found to follow the non-adiabatic hopping conduction in the high temperature range ($T > \theta_D/2$) and adiabatic hopping conduction mechanism in the low temperature ($T < \theta_D/2$) phase, while the Pb-doped La–Pb–Mn–O system showing SMT is found to follow the adiabatic hopping conduction mechanism for the entire temperature region (above SMT). Therefore, a change-over from the non-adiabatic to the adiabatic conduction regime occurs in the $LaMnO_3$ system caused by partially replacing La by Pb or other atoms (Ca, Br, Sr, etc). High temperature ($T > \theta_D/2$) conductivity data support the small-polaron hopping mechanism of Mott while variable range hopping conduction is followed by all the samples (doped or undoped) in the low temperature ($T_p < T < \theta_D/2$) region. The entire range of conductivity data above SMT cannot be fitted with the VRH model using the same value of $N(E_F)$. For the Pb-doped samples showing SMT, $N(E_F)$ is about two orders of magnitude higher than that of the undoped $LaMnO_3$ in the high temperature regime. In the low temperature regime $N(E_F)$ values are almost equal for all the samples (i.e., low temperature region near the SMT). The Seebeck coefficient of the Pb-doped $La_{1-x}Pb_xMnO_3$ (with $x = 0.1$) also supports the small-polaron hopping transport mechanism and showed appreciable magnetic field dependence near SMT. This suggests the importance of spin-ordering in the transport mechanism in these magnetic semiconductors which needs further investigation.

Acknowledgment

The authors are grateful to the Department of Science and Technology, Government of India, for a research grant to carry out the work.

References

[1] Mahendiran R, Tiwary S K, Roychaudhuri A K, Ramakrishnan T V, Mahesh R, Rangavittal N and Rao C N R 1996 *Phys. Rev.* B **53** 3348
[2] Peles A, Kunkel H P, Zhou X Z and Williams G 1999 *J. Phys.: Condens. Matter* **11** 8111
[3] Chen B, Rojo A G, Uher C, Ju H L and Greene R L 1997 *Phys. Rev.* B **55** 15471
[4] Ramarez A P 1997 *J. Phys.: Condens. Matter* **9** 8171 and references therein

[5] Jaime M, Salamon V, Pettit V, Rubinstein V, Treece R E, Horwitz J S and Chrisey D B 1996 *Appl. Phys. Lett.* **68** 1576
Jaime M, Salamon V, Pettit V, Rubinstein V, Treece R E, Horwitz J S and Chrisey D B 1996 *Phys. Rev.* B **54** 11914
[6] Hundley M F and Neumeier J J 1997 *Phys. Rev.* B **55** 11511
[7] Zener C 1951 *Phys. Rev.* **82** 403
[8] Park S H, Jeong Y H, Lee Ki-B and Kwon S J 1997 *Phys. Rev.* B **56** 67
[9] Ting C S, Chen X Y and Weng Z Y 1989 *Mod. Phys. Lett.* B **3** 1267
[10] Holstein T 1959 *Ann. Phys., NY* **8** 343
[11] Emin D and Holstein T 1963 *Ann. Phys., NY* **21** 439
[12] Mott N F and Davis E A 1971 *Electronics Processes in Noncrystalline Materials* (Oxford: Clarendon)
[13] Viret M, Ranno L and Coey J M D 1997 *Phys. Rev.* B **55** 8067
[14] Mahendiran R, Mahesh R, Raychaudhuri A K and Rao C N R 1995 *J. Phys. D: Appl. Phys.* **28** 1743
[15] Ji G, Fan X J, Zhang J H, Xiong C S and Li G 1998 *J. Phys. D: Appl. Phys.* **31** 3036
[16] Mandal P 2000 *Phys. Rev.* B **61** 14675
[17] Chatterjee S, Chou P H, Houg I P and Yang H D 2000 *Phys. Rev.* B **61** 6106
Hasanain S K, Nadeem M, Shah W H, Akbar M J and Hasan M M 2000 *J. Phys.: Condens. Matter* **12** 9007
[18] Goodenough J B 1963 *Magnetism and Chemical Bonds* (New York: Interscience)
[19] Crespi V H, Lu Li, Jia Y X, Khazeni K, Zetll A and Cohen M L 1996 *Phys. Rev.* B **53** 14 303
[20] Jia Y X, Lu Li, Khazeniu K, Yen D, Lee C S and Zettl A 1995 *Solid State Commun.* **94** 917
[21] Coey J M D, Viret M, Ranno L and Ounadjela K 1995 *Phys. Rev. Lett.* **75** 3910
[22] Sawicki M, Dietl T, Kossut J, Igalson J and Piesiewicz W 1986 *Phys. Rev. Lett.* **56** 508
[23] Kusters M R, Singleton J, Keen D, Greevy R Mc and Hayes W 1989 *Physica* B **155** 362
[24] Wang S, Li K, Chen V and Zhang Y 2000 *Phys. Rev.* B **61** 575
[25] Schnakenberg J 1968 *Phys. Status Solidi* **28** 623
[26] Emin D 1973 *Electronic Structure Properties of Amorphous Semiconductors* ed P G Le Comber and N F Mott (New York: Academic)
[27] Shimakawa K and Miyake K 1988 *Phys. Rev. Lett.* **61** 994
[28] Nakamura N and Eguchi E 1999 *J. Solid State Chemistry* **145** 56
Jung W H and Iguchi E 1996 *Phil Mag.* B **73** 873 and references therein
[29] Lukenheimer P, Resch M and Loidl A 1990 *Phys. Rev. Lett.* **69** 498
[30] Shames A I, Rozenberg E, Gorodeetski G, Pelleg J and Chaudhuri B K 1998 *Solid State Commun.* **107** 91
[31] Rozenberg E, Gorodetski G, Froumi N, Pelleg J, Polak M and Chaudhuri B K 1998 *J. Phys.* (France) **8** 359
[32] Chatterjee S, Banerjee S, Chaudhuri B K, Froumin N, Polak M and Baram J 1996 *Phys. Rev.* B **54** 10143
[33] Mott N F 1968 *J. Non-Cryst. Solids* **1** 1
[34] Austin G and Mott N F 1969 *Adv. Phys.* **18** 41
[35] Snyder G J, Hiskes R, DiCarolis V, Beasley M R and Geballe T H 1996 *Phys. Rev.* B **53** 14 434
[36] Chainani A, Mathew M and Sharma D D 1993 *Phys. Rev.* B **46** 9976
[37] Bogomolova L D, Dolgolenko T F, Lazukin V N and Filalova I V 1974 *Soviet Phys.–Solid State* **15** 2477
[38] Holstein T 1959 *Ann. Phys. (NY)* **8** 343
Kolber M A and MacCrone R K 1972 *Phys. Rev. Lett.* **29** 1457
Koffyberg F G and Benko F A 1980 *J. Non-Cryst. Solids* **40** 7
[39] Nakamura N and Eguchi E 1999 *J. Solid State Chem.* **58** 145
[40] Mostafa M, Boutiche S and Khodja M 1992 *Solid State Commun.* **82** 697
[41] Elliott S R 1983 *Physics of Amorphous Materials* (London: Longman) p 2912
[42] Gorham-Bergeron E and Emin D 1971 *Phys. Rev.* B **15** 360
[43] Zhang S 1996 *J. Appl. Phys.* **79** 4542
[44] Mahendiran R, Tiwary S K and RayChaudhuri A K 1996 *Solid State Commun.* **98** 701
[45] Ziese M and Srintiwarawong C 1998 *Phys. Rev.* B **58** 11 519
[46] Pi Li, Zheng Lei and Zhang Y 2000 *Phys. Rev.* B **61** 8917
Banerjee Aritra, Pal S, Bhattacharya S, Chaudhuri B K and Yang H D 2001 *Phys. Rev.* B **64** 104428